Article

Projected Hydroclimate Changes on Hispaniola Island through the 21st Century in CMIP6 Models

Dimitris A. Herrera [1,*] , **Rafael Mendez-Tejeda** [2] , **Abel Centella-Artola** [3] , **Daniel Martínez-Castro** [3] , **Toby Ault** [4] and **Ramón Delanoy** [5]

1   Instituto Geográfico Universitario, Universidad Autónoma de Santo Domingo,
Santo Domingo 10103, Dominican Republic

2   Research Laboratory in Atmospherical Science, University of Puerto Rico at Carolina,
Carolina 00984, Puerto Rico; rafael.mendez@upr.edu

3   Institute of Meteorology, Loma de Casa Blanca, Regla, La Habana 11700, Cuba;
abelcentella@gmail.com (A.C.-A.); danielmartinezc53@gmail.com (D.M.-C.)

4   Department of Earth, and Atmospheric Sciences, Cornell University, Ithaca, NY 14853, USA;
toby.ault@cornell.edu

5   Instituto de Física, Facultad de Ciencias, Universidad Autónoma de Santo Domingo,
Santo Domingo 51122, Dominican Republic; radelanoy@gmail.com

*   Correspondence: dherrera88@uasd.edu.do

Abstract: Climate change might increase the frequency and severity of longer-lasting drought in the Caribbean, including in Hispaniola Island. Nevertheless, the hydroclimate changes projected by the state-of-the-art earth system models across the island remain unknown. Here, we assess 21st-century changes in hydroclimate over Hispaniola Island using precipitation, temperature, and surface soil moisture data from the 6th Phase of the Coupled Model Intercomparison Project (CMIP6). The resulting analysis indicates, as with the previous 5th Phase of CMIP (CMIP5) models, that Hispaniola Island might see a significant drying through the 21st century. The aridity appears to be robust in most of the island following the Shared Socioeconomic Pathways (SSP) 5–8.6, which assumes the "worst case" greenhouse gas emissions into the atmosphere. We find a significant reduction in both annual mean precipitation and surface soil moisture (soil's upper 10 cm), although it appears to be more pronounced for precipitation (up to 26% and 11% for precipitation and surface soil moisture, respectively). Even though we provide insights into future hydroclimate changes on Hispaniola Island, CMIP6's intrinsic uncertainties and native horizontal resolution precludes us to better assess these changes at local scales. As such, we consider future dynamical downscaling efforts that might help us to better inform policy-makers and stakeholders in terms of drought risk.

Keywords: Hispaniola Island; Caribbean; climate change; climate models; CMIP6; drought

1. Introduction

Hispaniola Island, the second largest island in the Caribbean, is commonly affected by hydrometeorological events including droughts and tropical cyclones (e.g., [1–4]). Although tropical cyclones over Hispaniola Island demand attention due to their sudden and significant damage, severe and prolonged droughts also cause significant losses, especially in agriculture and tourism [1,2]. During the 2013–2016 Pan-Caribbean drought [4], for example, losses in agriculture exceeded $100 million [1], and put more than one million people into food insecurity risk, mostly in Haiti [1,2]. The 2013–2016 Pan-Caribbean drought is one of the most severe and costliest droughts on record that affected Hispaniola during the last 60 years [4]. Although this drought was associated with the strong El Niño between 2015 and 2016 [1,5,6], anthropogenic warming contributed to 13 ± 4% ($p < 0.05$) of its severity [4].

Previous studies suggest that the Caribbean region has experienced a trend towards aridity in the last 60 years [3,7]. However, although there is not a significant decrease

in rainfall, the opposite occurred in water evaporation, which is at least partially driven by higher temperatures [3,8,9]. In some parts of the Caribbean, in contrast, wetter conditions have been observed [3,9], including in some mountainous regions of Hispaniola Island. As previous studies suggest, local topographical gradients in islands like Hispaniola influence the severity and spatial variability of droughts in the Caribbean islands (e.g., [3,10–12]). Local topography interacts with regional atmospheric circulation and moisture transport, resulting in a heterogeneous distribution of precipitation [13]. Therefore, the spatial resolution of the climate and drought data available for Hispaniola and other Caribbean islands alike must be appropriate to capture the influence of topography on the severity of droughts at the local scale [3,11].

The fifth assessment report of the Intergovernmental Panel on Climate Change (IPCC) indicates that the Caribbean could experience a significant drying in the coming decades due to climate change [14]. Hispaniola Island might see up to 45% decreased rainfall during the summer (June–August), resulting in a significant water stress through the 21st century [14]. Additionally, the mean temperature in Hispaniola Island might likely increase up to 2–3.5 °C, compared to the current average (1986–2005) [14,15]. In fact, on the nearby island of Puerto Rico, the number of hot days doubled during the 1950–2014 period [16]. Higher temperatures contribute to higher evaporative demand from the atmosphere and consequently to a greater drought risk [17–19], even when rainfall remains unchanged concerning the current mean [18].

Like most Small Island Developing States (SIDS), Hispaniola Island is especially vulnerable to climate change due to the greater frequency and severity of extreme hydroclimate events, including droughts, projected through the 21st century [20,21]. Additionally, the rise in mean sea level, which could affect the coastal regions of the island, might result in more severe storm surges during the passage of tropical cyclones, as well as in the loss of underground aquifers due to saline contamination (e.g., [18]). Hispaniola Island is also vulnerable to drought due to its insular nature [18,21] as prolonged droughts often impact the whole island. Although water desalination programs are an option in some Caribbean states such as The Bahamas [22], the cost and maintenance of such technology would make it difficult for the island to be feasible.

Future aridity would represent an unprecedented challenge for the more than 25 million people expected to live on Hispaniola Island by 2050 [23], in terms of economic development, water availability, energy, and food security. It is, therefore, essential to understand and accurately assess drought risk in Hispaniola, in order to increase the island's capacity to adapt to the future aridity. This work evaluates the aridity projected in Hispaniola Island through the 21st century using archived climate model outputs of the 6th Phase of the Coupled Model Intercomparison Project (CMIP6; [24]). We aim to compare changes in the trends of simulated soil moisture and precipitation anomaly under different warming scenarios by 2100 in Hispaniola Island. To our knowledge, this is the first work on specifically evaluating 21st century hydroclimate change on Hispaniola Island using CMIP6 models.

2. Data and Methods

2.1. Study Area

Hispaniola Island (17.6°–20.0° N and 68.3°–74.5° W) is located in the Caribbean and shared by Haiti and the Dominican Republic (Figure 1). The island has an area of 76,192 km^2 and is the most populated in the Caribbean, with more than 21 million people [25]. As in many islands in the Caribbean, the annual precipitation cycle of Hispaniola has two maximums (April–May and August–October) and a minimum (November–March) (Figure 1). Between June and July, there is a relatively lower precipitation period consistent with the mid-summer drought (Figure 1a) [26] observed in the Caribbean and Central America [27–29]. However, because of topographical gradients, certain areas of the island experience slightly different annual cycles in precipitation and annual rainfall accumulations (Figure 1b). For example, in the northern and eastern portions of the island,

the wet season extends until late November because of the influence of synoptic-scale phenomena, such as frontal systems.
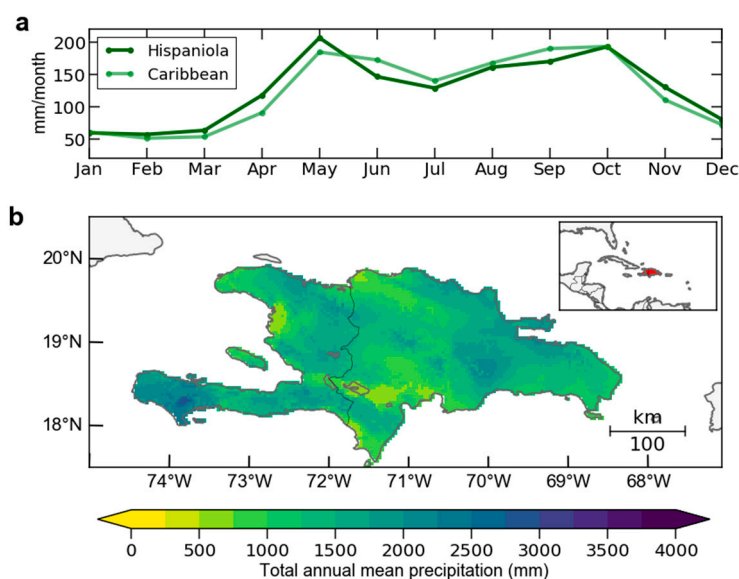
Figure 1. Observed precipitation climatology over Hispaniola Island: (**a**) Annual precipitation cycle of Hispaniola Island and the Caribbean for the 1950–2015 period, showing the two maximums (April–May and August–October), the minimum (November–March), and the mid-summer drought (June–July). (**b**) Total annual mean precipitation of Hispaniola Island showing spatial distribution in rainfall across the island. It is noticeable that there is a heterogeneous spatial distribution of precipitation, which is related with local topography. The data source comes from Herrera and Ault (2017) [3].

2.2. High-Resolution Climate Data

As reference observational data to compare against CMIP6 models, we used high-resolution precipitation and temperature products from Herrera and Ault [3]. This dataset spans 1950 to 2015 at 4 km (0.04°) horizontal resolution [3,4], and is available at https://ecommons.cornell.edu/handle/1813/58763. Herrera and Ault [3] built these climate products by statistically-downscaling the 7th version of the Global Precipitation Climatology Centre (GPCC; [30]) and the Berkeley Earth Surface Temperature (BEST; [31]), using WorldClim [32] and the Climate Hazards Group Infrared Precipitation with Station Data (CHIRPS; [33]). Herrera and Ault [3] have provided the details of the downscaling procedures to build these high-resolution gridded products, including the statistical methods used to downscale each climate variable and their validations. We used these downscaled products because most of the current observed gridded climate products available for Hispaniola Island and the Caribbean Islands have relatively coarse resolutions (e.g., ranging from 0.5° × 0.5° to 2° × 2°).

2.3. CMIP6 Data and Analysis

Table 1 enlists the CMIP6 models and climate variables we use in this work. We obtained the model data from https://esgfnode.llnl.gov/search/cmip6/ and bilinearly interpolated them to a common 1° × 1° horizontal resolution to conduct our analyses. We used fully-forced historical simulations for the 1950–2015 period, appended to the Shared Socioeconomic Pathways (SSP) 1-2.6 and 5-8.5 for 2015–2100. Historical simulations were forced from both natural and anthropogenic forcings, including anthropogenic greenhouse gas emissions and aerosols, volcanic eruptions, and orbital changes. In contrast to the Representative Concentration Pathways (RCP), SSPs represent emission scenarios based on socioeconomic projections through the 21st century [34,35]. For example, similar to the RCP8.5 in the previous CMIP's 5th Phase (CMIP5), the SSP5 assumes "the worst sce-

nario" pathway, while SSP1 assumes a significant reduction in current greenhouse gas emissions [34–36]. For most of the CMIP6 models, we selected the member r1i1p1f1, except for some models without this member (Table 1).

Table 1. Models used from the 6th Phase of the Coupled Model Intercomparison Project (CMIP6).

CMIP6 Model	Model Native Resolution	Historical				SSP1-2.6				SSP5-8.5			
		pr	mrsos	tas	evspsbl	pr	mrsos	tas	evspsbl	pr	mrsos	tas	evspsbl
ACCESS-CM2	0.80° × 0.53°	*	*	*	*	*	*	*	*	*	*	*	*
ACCESS-ESM1-5	0.80° × 0.53°	*	*	*	*	*	*	*	*	*	*	*	*
BCC-CSM2-MR	0.89° × 0.89°	*	*	*	*	*	*	*	*	*	*	*	*
CAMS-CSM1-0	0.89° × 0.89°	*	*	*	*	*	*	*	*	*	*	*	*
CanESM5	0.36° × 0.36°	*	*	*	*	*	*	*	*	*	*	*	*
CESM2	1.07° × 0.80°	*	*	*	x	*	*	*	x	*	*	*	x
CESM2-WACCM	1.07° × 0.80°	*	*	*	x	*	*	*	x	*	*	*	x
CNRM-CM6-1 **	0.71° × 0.71°	*	*	*	*	*	*	*	*	*	*	*	*
FGOALS-f3	1.0° × 0.80°	*	*	*	*	*	*	*	*	*	*	*	*
GFDL-ESM4	1.0° × 0.80°	*	*	*	x	*	*	*	x	*	*	*	x
GISS-E2-1-G	0.50° × 0.40°	*	*	*	*	*	*	*	*	*	*	*	*
HadGEM3-GC31-LLa	0.80° × 0.53°	*	*	*	*	*	x	*	x	*	x	*	*
INM-CM5-0	0.67° × 0.50°	*	x	*	x	*	x	*	*	*	x	*	x
IPSL-CM6A-LR	0.80° × 0.40°	*	*	*	*	*	*	*	*	*	*	*	*
MIROC-ES2L **	0.36° × 0.36°	*	*	*	*	*	*	*	*	*	*	*	*
MIROC6	0.71° × 0.71°	*	x	*	*	*	x	*	*	*	x	*	*
MPI-ESM1-2-LR	0.53° × 0.53°	*	x	*	*	*	x	*	*	*	x	*	*
MRI-ESM2-0	0.89° × 0.89°	*	*	*	*	*	*	*	*	*	*	*	*

Acronyms: pr (precipitation), mrsos (moisture content of soil layer), tas (air temperature), evspsbl (water evaporation flux), SSP (Shared Socioeconomic Pathways). The CMIP6's variables we use are marked by an asterisk (*), while boxes marked with "x" indicate that this file is not currently available. Two asterisks (**) indicates the use of model members other than r1i1p1f1.

To ensure the use of CMIP6 data solely over Hispaniola Island, we implemented the following steps: (1) we selected and extracted CMIP6 data over Hispaniola Island (e.g., 17.6°–20.0° N and 68.3°–74.5° W). By selecting the area bounded by specific latitudes and longitudes, we ensured that we were working over Hispaniola Island and not elsewhere in the Caribbean. (2) We regridded (interpolated) CMIP6 data to a 1° × 1° resolution (including the model's land-mask) to calculate multimodel ensemble means. (3) We conducted the statistical analysis of this work, including the computation of long-term means, anomalies, standard deviations, trends, and statistical significance to all the CMIP6 models we used. (4) Finally, we interpolated the resulting (processed) data to a 4 km horizontal resolution, solely for display purposes.

2.4. Soil Moisture and Precipitation Trends

We calculated the trends of surface soil moisture and precipitation anomalies for each CMIP6 model and the SSP1-2.6 and SSP5-8.5 scenarios. However, because of the inherent differences of soil moisture and precipitation as drought indicators, in addition to differences in CMIP6 parameterization and numerical schemes, we first converted their anomalies into z-scores following Ault et al. (2014) [37]:

$$z = \frac{x - \overline{x}}{\sigma} \tag{1}$$

where z is the normalized drought indicator time series, x is the original drought indicator time series, $\overline{x}$ is the long-term mean for the 1950–2015 period, and σ is the standard deviation. We calculated the trends using the linear best-fit and spline methods. While the linear trend might be appropriate for monthly time series spanning fifty or fewer years, this approach might not be sensitive to sub-decadal changes in soil moisture and

precipitation during the last decades [38]. The spline method, as with other low-pass filters, solves this limitation by capturing these sub-decadal trends.

2.5. Statistical Significance

We used a two-tailed *t*-test to calculate the statistical significance of the differences between trends from each SSP scenario. Here our null-hypothesis states that "there is no difference in soil moisture and precipitation anomalies between the SSP1-2.6 and SSP5-8.5 warming scenarios." We selected the mean as the statistic to test using the soil moisture and precipitation anomalies of SSP1-2.6 and compared them against the same variables but for SSP5-8.5 through the 21st century. We considered as significant change those with p values ≤ 0.05 at the 95% confidence level.

3. Results

3.1. Observed and Simulated Climatologies

The CMIP6 models we use in this work (Table 1) simulate reasonably well the annual precipitation cycle in Hispaniola Island, including the existence of the midsummer-drought (Figure 2a). However, the midsummer-drought is more noticeable by 2100 following both the SSP1-2.6 and SSP5-8.5 warming scenarios, as compared to the historical period (1950–2015) (Figure 2a). As in previous CMIP model generations (e.g., [39,40], CMIP6 models underestimate precipitation in the Caribbean and Hispaniola Island. According to Ryu and Hayhoe (2014) [40], this may be due to the cold-bias in sea surface temperatures shown by most global climate models. The total annual precipitation from the CMIP6 multimodel mean is, on average, 989 mm/year over land in Hispaniola Island. This is 494 mm lower than the annual mean from the downscaled 7th version of GPCC product we use (1483 mm/year) (Figure 2a).
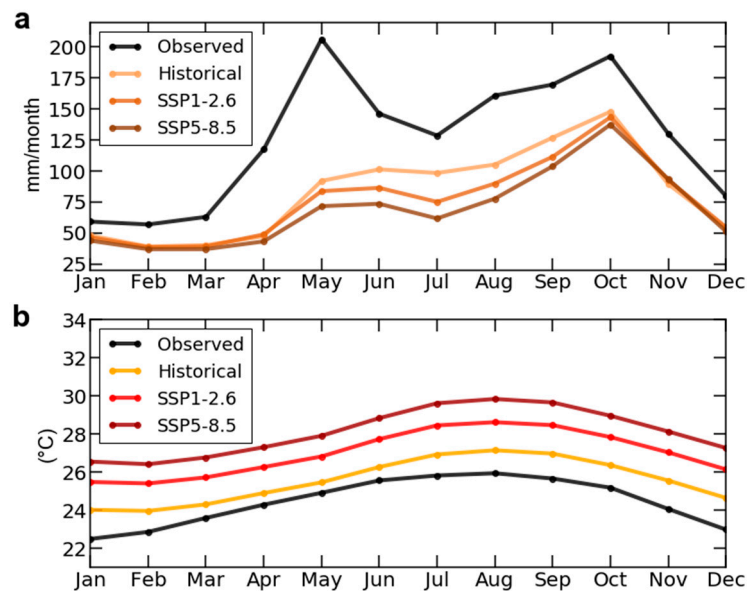
Figure 2. Observed and modeled annual cycles in precipitation and temperature in Hispaniola Island. (1950–2015). (**a**) Annual cycles in precipitation from observations (Herrera and Ault, 2017 [3]), and CMIP6's historical and projected simulations following the SSP1-2.6 and SSP5-8.5 warming scenarios. (**b**) as panel (**a**) but for the annual temperature cycle.
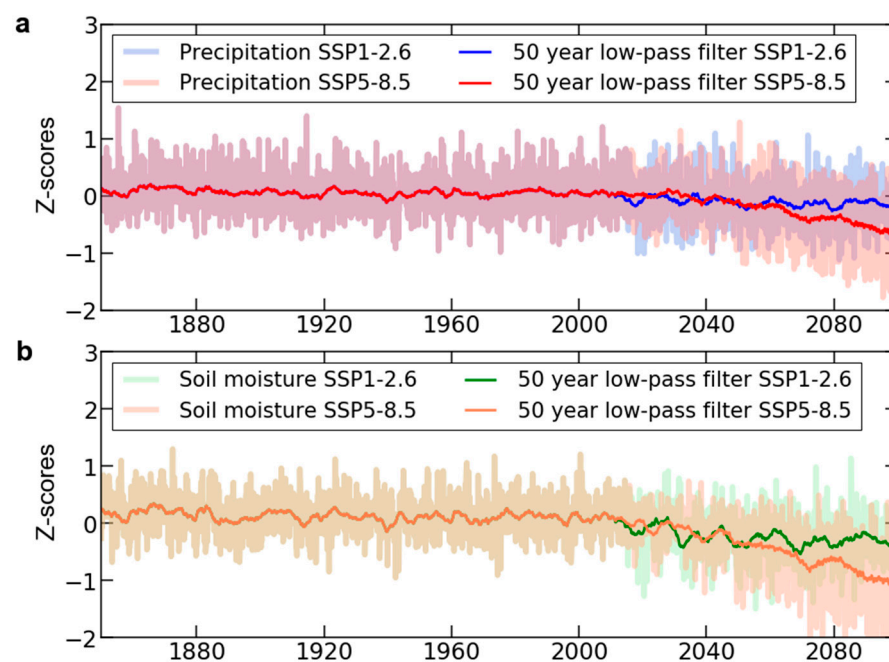
Projected changes in the precipitation annual cycle in Hispaniola Island are more likely to occur in the total annual means rather than changes in the seasonality. By the end of the 21st century (2050–2100), for example, climate models indicate an 80 mm decrease in annual precipitation following the SSP1-2.6 scenario and 158 mm less rain following the SSP5-8.5 in comparison to the model historical period (1950–2015). These changes represent an 8 and 16% decrease in total annual precipitation, respectively, as compared to

the historical period in CMIP6. The greatest decrease in precipitation might occur during the boreal summer (June–August), especially in July, with 23 and 37% less rain following the SSP1-2.6 and SSP5-8.5 warming scenarios, respectively (Figure 2a).

In contrast to precipitation, CMIP6 models overestimate the annual mean temperature in Hispaniola Island. The multimodel mean for annually averaged temperature is 1.1 °C higher than the observed temperature mean from the downscaled BEST product for the same period (e.g., 24.4 °C vs. 25.5 °C) (Figure 2b). Following the SSP1-2.6 warming scenario, the annual mean temperature for the Island might be 1.5 °C higher than during the modeled historical period. However, following the SSP5-8.5 scenario, a 2.6 °C increase in annual mean temperature is projected by the end of the 21st century on Hispaniola Island (Figure 2b).

### 3.2. Observed and Simulated Historical Trends

The observed precipitation trend between 1950 and 2015 on Hispaniola Island is −0.86 mm/decade. However, this trend is not-significant ($p > 0.05$). Historical simulations from CMIP6 multimodel ensemble also suggest a not-significant trend toward dryness (−0.01 mm/decade) for the 1950–2015 period (Figure 3a). In contrast, there is a significant decrease in precipitation through the 21st century following the SSP5-8.5, with −2.22 mm/decade, while it is not-significant following the SSP1-2.6 scenario. Trends in modeled superficial soil moisture are consistent with those in precipitation. For the historical period, there is not a significant trend toward aridity, with −0.08 mm/decade ($p > 0.05$). However, and as opposed to modeled precipitation trends, both SSP1-2.6 and SSP5-8.5 warming scenarios suggest a significant decline in surface soil moisture through the 21st century, with rates ranging from −0.13 to −0.36 mm/decade, respectively ($p < 0.05$) (Figure 3b).

Figure 3. Multi-model means of projected changes in precipitation and surface soil moisture. (**a**) Trends of precipitation following the SSP1-2.6 and SSP5-8.5 warming scenarios. (**b**) as in (a) but for surface soil moisture (soil's upper 10 cm). For display purposes, for each climate variable, we appended historical simulations (1850–2015) to each of the projected simulations following the SSP1-2.6 and SSP5-8.5 warming scenarios (2015–2100).

Since at least 1950, Hispaniola Island has seen a steady and significant increase in surface mean temperature, trending 0.14 °C/decade on average. All CMIP6 models used in this work are consistent with the trends found from instrumental records, and suggest

a significant warming across the island in the 21st century, even following the lowest greenhouse gas emission scenarios (Figure 4a). Historical simulations from CMIP6's multimodel mean indicate a warming trend of 0.05 °C/decade, whereas the projected trends are 0.05 °C/decade and 0.25 °C/decade, for SSP1-2.6 and SSP5-8.5, respectively. Water evaporation flux is also projected to change though the 21st century, although not as significantly as precipitation and temperature. Following the SSP1-2.6 warming scenario, for example, the multimodel ensemble trend is near zero and not-significant. In contrast, an small increase in water evaporation is projected following the SSP5-8.5 scenario, with 0.05 mm/decade (Figure 4b).
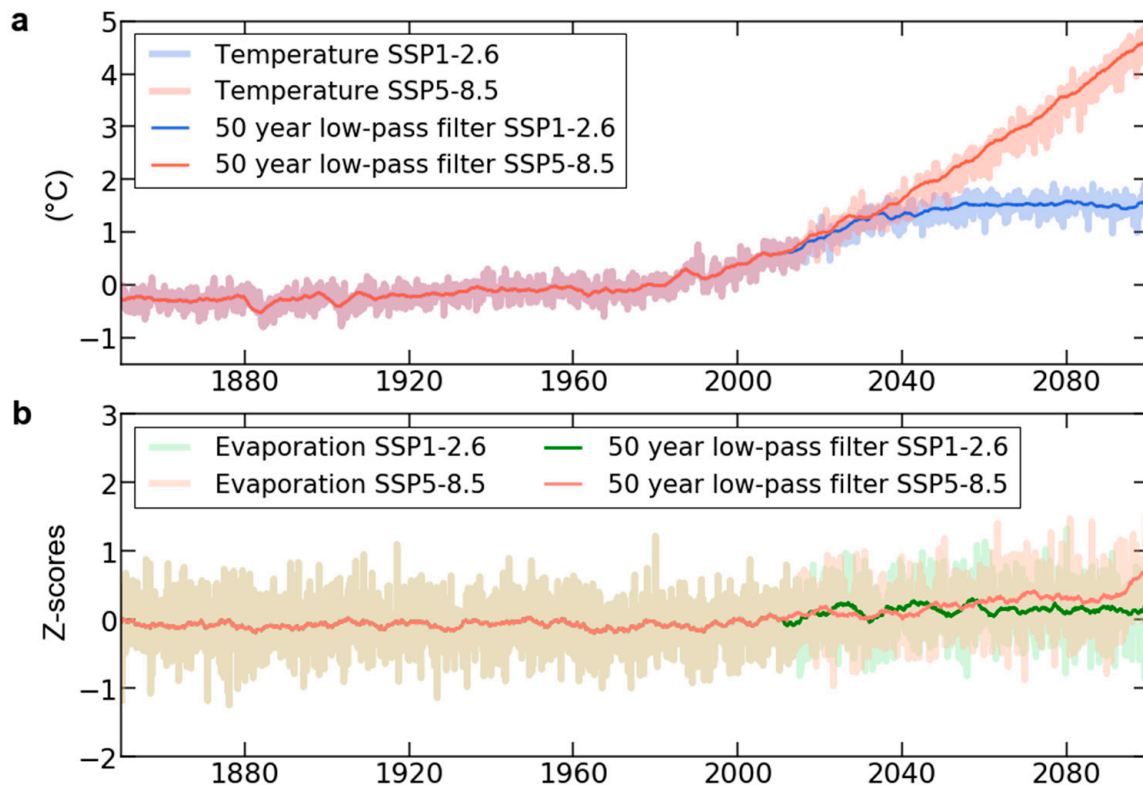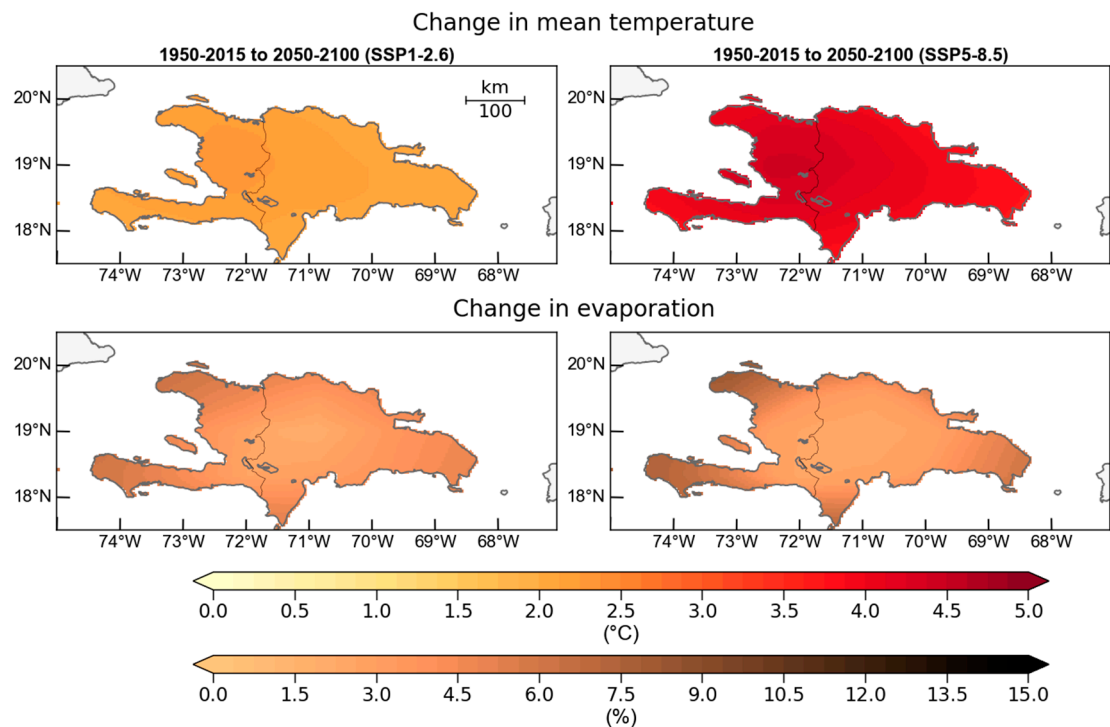

Figure 4. Multimodel means of projected changes in temperature and evaporation. (**a**) Trends of temperature following the SSP1-2.6 and SSP5-8.5 warming scenarios. (**b**) as in (a) but for evaporation. For display purposes, for each climate variable, we appended historical simulations (1850–2015) to each of the projected simulations following the SSP1-2.6 and SSP5-8.5 warming scenarios (2015–2100).

3.3. Projected Changes in Precipitation and Soil Moisture

Hydroclimate changes by the end of the 21st century (e.g., 2050–2100) as a result of anthropogenic climate change are not homogeneous across the island. Despite the relatively coarse horizontal resolution of CMIP6 models (Figures 5 and 6), we find that certain areas of Hispaniola Island may see drier conditions than others, as compared to the historical period (e.g., 1950–2015) (Figure 5). For example, the CMIP6 multimodel mean suggests a decrease of up to 26% in precipitation over southeastern Hispaniola Island, following the SSP5-8.5 scenario, whereas up to 11% decreased rainfall is suggested with the SSP1-2.6 scenario, again, in southeastern Hispaniola (Figure 5). Changes in annual mean in surface soil moisture is consistent with changes in precipitation. However, the magnitude of the drying in surface soil moisture is lower than in precipitation, with up to 9% decrease in soil moisture with the SSP5-8.5 scenario and 3% lower moisture with the SSP1-2.6 (Figure 5). In contrast to precipitation, the highest decline in surface soil moisture may occur in the central-west portion of Hispaniola and a small area on the eastern side of the island.
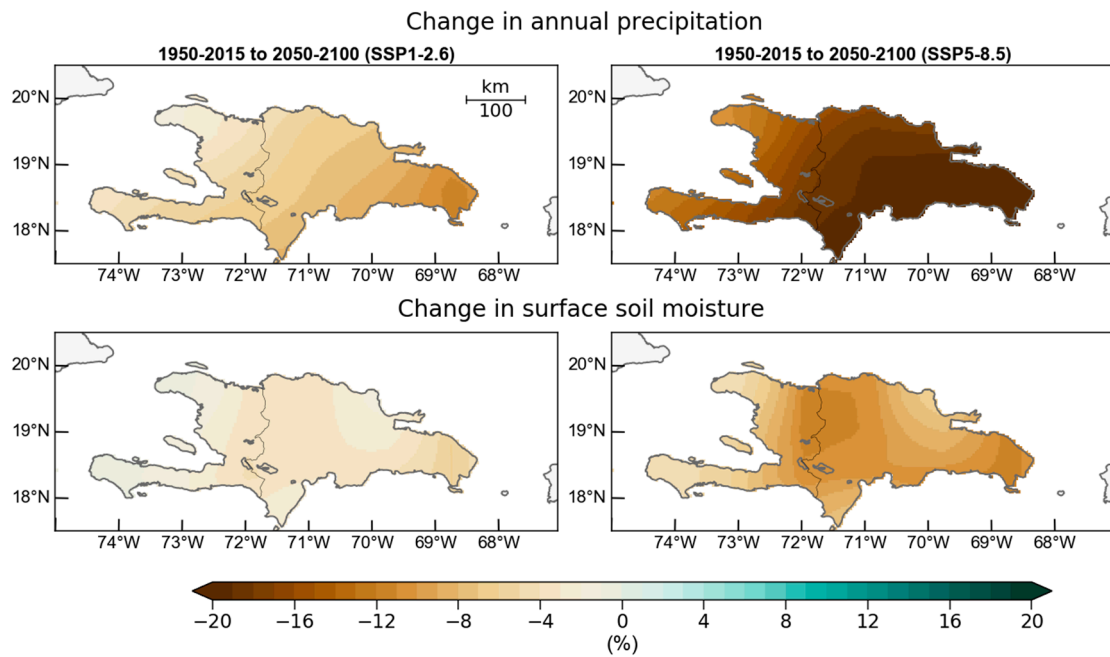
Figure 5. Multimodel means of the projected changes in precipitation and surface soil moisture on Hispaniola Island from CMIP6: Upper panels show the changes in the annual precipitation following the shared socioeconomic pathway (SSP) 1–2.6, which assumes a sharp decrease in greenhouse gas emissions in the left, and 5–8.5, which assumes the current emission rates of greenhouse gases in the right. For display purposes, we bilinearly interpolated the results to a common $0.04° \times 0.04°$ (4 km) horizontal resolution to match with our high-resolution products.

Figure 6. Multimodel means of the projected changes in surface temperature and water evaporation flux on Hispaniola Island from CMIP6. The upper panels show the changes in surface temperature following the shared socioeconomic pathway (SSP) 1–2.6 to the left, and SSP 5–8.5 to the right. For display purposes, we bilinearly interpolated the results to a common $0.04° \times 0.04°$ (4 km) horizontal resolution to match with our high-resolution products.

Changes in the projected temperatures means are relatively homogeneous (Figure 6). In certain areas of Hispaniola Island, an increase of up to 4.4 °C is projected by climate models by the end of the 21st century following the SSP5-8.5 scenario. This projection is slightly smaller under the SSP1-2.6 warming scenario, with a projected increase in temperature of 2.3 °C (Figure 6). Conversely, changes in the annual mean water evaporation may see up to 6.3% increase with SSP1-2.6, and 10.2% following the SSP5-8.5 warming scenario (Figure 6). Based on the CMIP6 models we use, the central portion of Hispaniola Island is expected to see the lowest increases in water evaporation, whereas the west portion (western Haiti) may see the greatest change (Figure 6).

4. Discussion

Consistent with the previous generations of global climate models (i.e., CMIP3 and CMIP5), CMIP6 models indicate a significant trend toward aridity in the Caribbean through the 21st century, including on Hispaniola Island. We find that precipitation changes across the island are mainly driven by a significant decline in the summer rainfall (May–October), even though the seasonality might not change that much (Figure 2a). However, it is noteworthy to mention that, following either the worst emission scenario or drastically reducing greenhouse gas emissions, climate models suggest that Hispaniola Island might have a more pronounced midsummer drought by the end of the 21st century. Although the dynamical causes of this projection are not yet well understood, Taylor et al. [41] suggest that this might be due to an increase in the intensity of the Caribbean Low-Level Jet (CLLJ), which is a conveyor that advects moisture from the Caribbean Sea to Central America and the Gulf of Mexico [42]. A stronger CLLJ also correlates with a stronger North Atlantic subtropical high (NASH), as observed during the mid-summer drought [39]. These findings are consistent with the previous CMIP generations (e.g., [39]), which suggest an intensification of the mid-summer drought through the 21st century due to the intensification and westward expansion of the NASH [39]. However, from our results, we cannot say that these dynamical mechanisms underpin the aridity projected for Hispaniola Island in CMIP6 models. Answering this question requires us to first evaluate the skill of current CMIP6 models in simulating major dynamical features of drought on Hispaniola Island and the Caribbean islands alike, and second, to analyze how these features might change through the 21st century, as refs. [39,40] did for CMIP3 and CMIP5, respectively.

Even though a decline in precipitation in Hispaniola Island is robust across different models, the response of surface soil moisture is less pronounced (Figures 5 and 7). For example, while precipitation rates may fall up to 89 mm/decade between 2015 and 2100, the surface soil moisture content declines by up to 36 mm/decade. These findings open the question of whether this may be due to the effects of plants' water use efficiency as a result of increased CO_2 concentrations in the atmosphere (e.g., [43]). More efficient water use by plants could, theoretically, decrease water evaporation rates. Therefore, we might see a less pronounced trend in water evaporation as compared to surface temperature and other variables, such as wind speed and net radiation. Even though we find such a result in this work (e.g., Figures 4 and 6), we emphasize that uncertainties in these projections arise due to several reasons, including feedbacks from vegetation processes [44,45], and the parameterization of hydrologic and other surface processes in CMIP6 models. For example, it is not yet clear how earth system models represent many hydrologic processes on a single or a few grid-cells (e.g., surface runoff), which is how some CMIP6 models (e.g., the Canadian Earth System Model version 5 [CanESM5]) represent some of the Caribbean Islands, including Hispaniola Island.
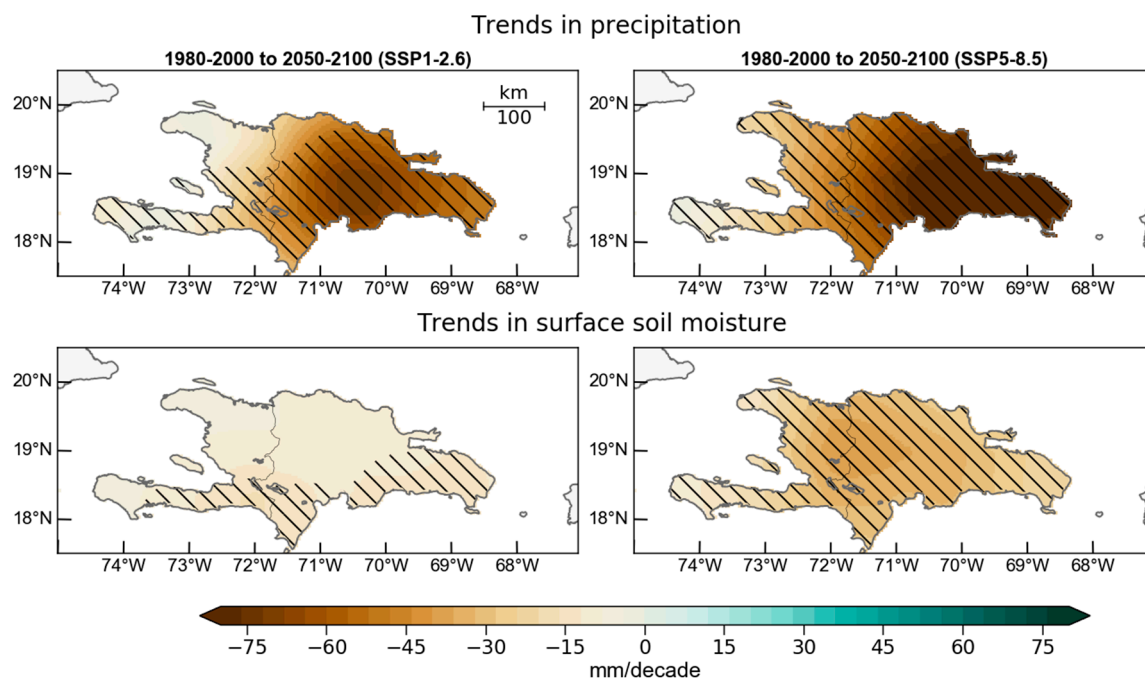
Figure 7. CMIP6 multimodel means of decadal trends in precipitation and surface soil moisture on Hispaniola Island. Hatching represents areas with statistically significant trends at the 95% interval. For display purposes, we bilinearly interpolated the results to a common $0.04° \times 0.04°$ (4 km) horizontal resolution to match with our high-resolution products.

We also speculate that other physical factors, such as an increase in extreme hydroclimate events (i.e., extreme precipitation and droughts [46]), may at least partly explain a higher decline in rainfall than in surface soil moisture. For example, consider an extreme precipitation event after a prolonged drought. Since soil's infiltration capacity may be reduced (especially in clayish soils), we should expect an increased runoff and relatively higher surface soil moisture content as compared to the deeper soil layers. It would make sense, then, to observe a more pronounced drying in total column soil moisture than in its surface counterpart. As suggested by ref. [45], there is indeed a marked drying in the Caribbean and Central America in total column soil moisture in CMIP6 models through 21st century, which agrees with our explanation for Hispaniola Island. However, we probably need regional climate modeling (e.g., dynamical downscaling) to have a more accurate answer to this question.

In addition to the intrinsic uncertainties in CMIP6 models (e.g., in representations of hydrologic and vegetation processes), because of their relatively coarse resolution, these models might underestimate the effects of dynamical and thermodynamical processes that occur at local scales in the Caribbean islands [3,13,29]. This limitation might, in turn, impact the models' accuracy of future hydroclimate projections on Hispaniola Island. As shown in Figure 8, for example, the intermodel spread suggests a better agreement in surface temperature during the historical period and the first 35 years following both SSP1-2.6 and SSP5-8.5 warming scenarios (i.e., until ~2050). From 2050, however, these projections are more uncertain, which is consistent with surface temperature projections at regional and global scales [14,45,47]. In contrast, intermodel spreads of precipitation, soil moisture, and water evaporation flux are significantly higher than temperature, again similar to regional and global projections. Provided that Hispaniola Island is represented by a few grid cells in CMIP6 models, the similarities with regional climate change projections may be due to the relatively coarse horizontal resolution of the CMIP6 models we used.
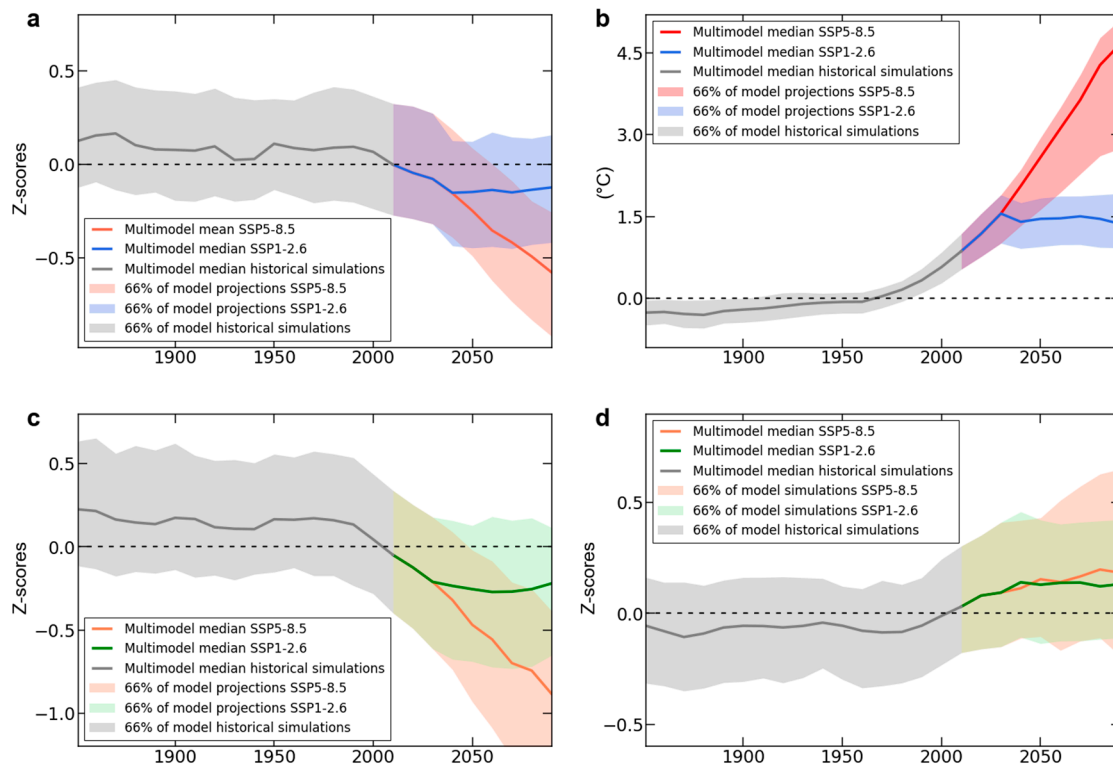
Figure 8. CMIP6's median intermodel spread and median of (**a**) precipitation, (**b**) surface temperature, (**c**) surface soil moisture (soil's top 10 cm), and (**d**) water evaporation flux. The colored shaded areas represent the interquartile range of the models' projections (bounded by the 17th and 83rd percentiles), while the solid lines represent the multimodel median for historical simulations (1850–2015), and SSP1-2.6 and SSP5-8.5 (2015–2100). All time series were smoothed using moving mean of 10 years.

Although our results suggest spatially-heterogeneous hydroclimate projections for Hispaniola Island (e.g., a more pronounced drying in the southeastern portion of the island), this variability is not strictly due to local topography. Instead, it might have a strong influence on processes occurring over (the model) ocean. We thus consider that dynamically-downscaling efforts of CMIP6 model outputs (as in refs. [48–50]) is a plausible option to help us to better understand the projected hydroclimate changes on Hispaniola Island at local scales. Previous statistical downscaling efforts of future climate projections have done a good job in capturing the effects of local topography [51]. However, the scarcity (or even the lack) of instrumental records of hydroclimate variables (e.g., long-term observations of soil moisture) precludes us from using statistical downscaling methods. We thus propose the use of dynamical downscaling over statistical downscaling methods to increase CMIP6 model resolution for Hispaniola Island and other small islands of the Caribbean region.

5. Conclusions

We have assessed the hydroclimate changes projected on Hispaniola Island through the 21st century as a result of increasing anthropogenic greenhouse gases in the atmosphere. We provide insights into the hydroclimate changes that the island might face through the 21st century as a result of anthropogenic climate change. We find a significant trend toward aridity, mainly driven by a robust decline in annual mean precipitation, which further manifested as reduced surface soil moisture. The aridity projected by climate models in precipitation is more pronounced than that in surface soil moisture. We speculate that it might be due to several factors, including feedback from vegetation processes and the horizontal resolutions of the current earth system models. These findings are similar to previous work using CMIP3 and CMIP5 for the Caribbean (e.g., [39,40]), and, as suggested

in ref. [45], CMIP6 models might be subject to similar uncertainties as CMIP5 models, especially in the projections of precipitation and vegetation processes.

Even though this work provides insights into the future hydroclimate changes on Hispaniola Island, higher resolution climate model data are required to better assess hydroclimate changes at local scales, which might be more useful for stakeholders and policy-makers. This is critical, for example, to understand how Hispaniola's complex topography changes (or not) moisture fluxes locally (e.g., [29]). As such, dynamical downscaling from regional climate modeling efforts presents a plausible option. Importantly, processes related to local topography (e.g., [13]) and the size of the island itself [52] are not resolved by the current CMIP6 models, and they have been shown to modulate hydroclimate variability at local scales (e.g., [3,13]). Finally, future fresh water availability in Hispaniola Island might be at risk due to both increased aridity and salt-water intrusion into aquifers [21]. This work provides the initial insights for the island in terms of hydroclimate changes through the 21st century, which may help stakeholders and decision-makers to better prepare for the future aridity on the island.

Author Contributions: D.A.H. conceived the idea of this work. D.A.H., R.M.-T., A.C.-A., T.A., D.M.-C., R.D. obtained and analyzed the data. D.A.H. wrote and prepared the manuscript. All authors have read and agreed to the published version of the manuscript.

Institutional Review Board Statement: Not applicable.

Informed Consent Statement: Not applicable.

Data Availability Statement: The model data used in this work is available at https://esgfnode.llnl.gov/search/cmip6/; while the observational data can be found at https://ecommons.cornell.edu/handle/1813/58763.

Conflicts of Interest: The authors declare no conflict of interest.

References

1. OCHA. *Drought in Central America in 2015: Situation Report (as of October 6, 2015)*; United Nations Office for the Coordination of Humanitarian Affairs (OCHA): New York, NY, USA, 2016; Available online: https://reliefweb.int/report/guatemala/drought-central-america-2015-situation-report-october-6-2015 (accessed on 1 November 2016).
2. FAO. *Situation Report: Dry Corridor in Central America*; Food and Agriculture Organization of the United Nations: Rome, Italy, 2016; p. 3. Available online: http://www.fao.org/emergencies/resources/documents/resources-detail/en/c/422097/ (accessed on 1 November 2016).
3. Herrera, D.A.; Ault, T.R. Insights from a new high-resolution drought atlas for the Caribbean spanning 1950–2016. *J. Clim.* **2017**, *30*, 7801–7825. [CrossRef]
4. Herrera, D.A.; Ault, T.R.; Fasullo, J.T.; Coats, S.J.; Carrillo, C.M.; Cook, B.I.; Williams, A.P. Exacerbation of the 2013–2016 Pan-Caribbean drought by anthropogenic warming. *Geophys. Res. Lett.* **2018**, *45*, 10619–10626. [CrossRef] [PubMed]
5. Blunden, J.; Arndt, D.S. State of the Climate in 2015. *Bull. Amer. Meteor. Soc.* **2016**, *97*, S1–S275. [CrossRef]
6. Hernández Ayala, J.J. Atmospheric teleconnections and their effects on the annual and seasonal rainfall climatology of Puerto Rico. *Theor. Appl. Climatol.* **2019**, *137*, 2915–2925. [CrossRef]
7. Neelin, J.D.; Münnich, H.; Su, H.; Meyerson, J.E.; Holloway, C.E. Tropical drying trends in global model and observations. *Proc. Natl. Acad. Sci. USA* **2006**, *103*, 6110–6115. [CrossRef]
8. Jones, P.D.; Harpham, C.; Harris, I.; Goodess, C.M.; Burton, A.; Centella-Artola, A.; Taylor, M.A.; Bezanilla-Morlot, A.; Campbell, J.D.; Stephenson, T.S.; et al. Long-term trends in precipitation and temperature across the Caribbean. *J. Int. Climatol.* **2015**, *36*, 3314–3333. [CrossRef]

9. Stephenson, T.S.; Vincent, L.A.; Allen, T.; Van Meerbeeck, C.J.; McLean, N.; Peterson, T.C.; Taylor, M.A.; Aaron-Morrison, A.P.; Auguste, T.; Bernard, D.; et al. Changes in extreme temperature and precipitation in the Caribbean region, 1961–2010. *Int. J. Climatol.* **2014**, *34*, 2957–2971. [CrossRef]

10. Izzo, M.; Rosskopf, C.M.; Aucelli, P.C.; Maratea, A.; Méndez, R.; Pérez, C.; Segura, H. A new climatic map of the Dominican Republic based on the Thornthwaite classification. *Phys. Geogr.* **2010**, *31*, 455–472. [CrossRef]

11. Torres-Valcárcel, A.R. Teleconnections between ENSO and rainfall and drought in Puerto Rico. *Int. J. Climatol.* **2018**, *38*, e1190–e1204. [CrossRef]

12. Jury, M.R.; Bernard, D. Climate trends in the East Antilles Islands. *Int. J. Climatol.* **2020**, *40*, 36–51. [CrossRef]

13. Smith, R.B.; Minder, J.R.; Nugent, A.D.; Storelvmo, T.; Kirshbaum, D.J.; Warren, R.; Lareau, N.; Palany, P.; James, A.; French, J. Orographic Precipitation in the Tropics: The Dominica Experiment. *Bull. Amer. Meteor. Soc.* **2012**, *93*, 1567–1579. [CrossRef]

14. IPCC. *Climate Change 2014: Synthesis Report*; Pachauri, R.K., Meyer, L.A., Eds.; IPCC: Geneva, Switzerland, 2014; p. 151.

15. Karmalkar, A.V.; Bradley, R.S.; Diaz, H.F. Climate change in Central America and Mexico: Regional climate model validation and climate change projections. *Clim. Dyn.* **2011**, *37*, 605. [CrossRef]

16. Méndez-Tejeda, R. Increase in the Number of Hot Days for Decades in Puerto Rico 1950–2014. *Environ. Nat. Res. Res.* **2017**, *7*, 16–26. [CrossRef]

17. Cook, B.I.; Ault, T.R.; Smerdon, J.E. Unprecedented 21st century drought risk in the American Southwest and Central Plains. *Sci. Adv.* **2015**, *1*, e1400082. [CrossRef] [PubMed]

18. Ault, T.R.; Mankin, J.S.; Cook, B.I.; Smerdon, J.E. Relativeimpacts of mitigation, temperature, and precipitation on 21st-century megadrought risk in the American Southwest. *Sci. Adv.* **2016**, *2*, e1600873. [CrossRef] [PubMed]

19. Ault, T.R. On the essentials of drought in a changing climate. *Science* **2020**, *368*, 256–260. [CrossRef]

20. Centella-Artola, A.; Bezanilla, A.; Leslie, K.R. *A Study of the Uncertainty in Future Caribbean Climate Using the PRECIS Regional Climate Model*; Caribbean Community Climate Change Centre (CCCCC): Belmopan, Belize, 2008.

21. Karnauskas, K.B.; Schleussner, C.F.; Donelly, J.P.; Anchukaitis, K.J. Freshwater stress on small island developing states: Population projections and aridity changes at 1.5 and C. *Reg. Environ. Chang.* **2018**, *18*. [CrossRef]

22. UNESCO; Programa Hidrológico Internacional (PHI). The use of desalination plants in the Caribbean. *Tech. Rep.* **2006**. Available online: http://unesdoc.unesco.org/images/0022/002281/228110e.pdf (accessed on 1 November 2016).

23. United Nations, Department of Economic and Social Affairs, Population Division. *World Population Prospects 2019: Data Booket*; ST/ESA/SER.A/424; United Nations, Department of Economic and Social Affairs, Population Division, 2019; Available online: https://population.un.org/wpp/ (accessed on 1 October 2020).

24. Eyring, V.; Bony, S.; Meehl, G.A.; Senior, C.; Stevens, B.; Stouffer, R.J.; Taylor, K.E. Overview of the Coupled Model Intercomparison Project Phase 6 (CMIP6) experimental design and organisation. *Geosc. Mod. Dev. Dis.* **2016**, *8*, 1937–1958. [CrossRef]

25. Central Intelligence Agency. *The World Factbook 2020*; Central Intelligence Agency: Washington, DC, USA, 2020.

26. Magaña, V.; Amador, J.; Medina, S. The midsummer drought over Mexico and Central America. *J. Clim.* **1999**, *12*, 1577–1588. [CrossRef]

27. Anderson, T.G.; Anchukaitis, K.J.; Pons, D.; Taylor, M. Multiscale trends and precipitation extremes in the Central American Midsummer Drought. *Environ. Res. Lett.* **2019**, *14*, 124016. [CrossRef]

28. Alfaro, E.; Hidalgo, H.; Alfaro-Córdoba, M. Aridity Trends in Central America: A Spatial Correlation Analysis. *Atmosphere* **2020**, *11*, 427. [CrossRef]

29. Herrera, D.A.; Ault, T.R.; Carrillo, C.M.; Fasullo, J.T.; Li, X.; Evans, C.P.; Alessi, M.J.; Mahowald, N.M. Dynamical characteristics of drought in the Caribbean from observations and simulations. *J. Clim.* **2020**, *33*, 10773–10797. [CrossRef]

30. Schneider, U.; Becker, A.; Finger, P.; Meyer-Christoffer, A.; Rudolf, B.; Ziese, M. GPCC Full Data Reanalysis Version 7.0 at 1.0°: Monthly Land-Surface Precipitation from Rain-Gauges Built on GTS-Based and Historic Data. 2015. Available online: https://opendata.dwd.de/climate_environment/GPCC/html/fulldata_v7_doi_download.html (accessed on 22 December 2020). [CrossRef]

31. Rohde, R.; Muller, R.A.; Jacobsen, R.; Muller, E.; Perlmutter, S.; Rosenfeld, A.; Wurtele, J.; Groom, D.; Wickham, C. A new estimate of the average Earth surface land temperature spanning 1753 to 2011. *Geoinfo. Geostat. Over.* **2013**, *1*. [CrossRef]

32. Hijmans, R.J.; Cameron, S.E.; Parra, J.L.; Jones, P.G.; Jarvis, A. Very high resolution interpolated climate surfaces for global land areas. *Int. J. Climatol.* **2005**, *25*, 1965–1978. [CrossRef]

33. Funk, C.; Peterson, P.; Landsfeld, M.; Pedreros, D.; Verdin, J.; Shukla, S.; Husak, G.; Rowland, J.; Harrison, L.; Hoell, A.; et al. The climate hazards infrared precipitation with stations—a new environmental record for monitoring extremes. *Sci. Data* **2015**, *2*, 150066. [CrossRef] [PubMed]

34. O'Neill, B.C.; Tebaldi, C.; Van Vuuren, D.P.; Eyring, V.; Friedlingstein, P.; Hurtt, G.; Knutti, R.; Kriegler, E.; Lamarque, J.F.; Lowe, J.; et al. The Scenario Model Intercomparison Project (ScenarioMIP) for CMIP6. *Geosci. Model Dev.* **2016**, *9*, 3461–3482. [CrossRef]

35. Riahi, K.; Van Vuuren, D.P.; Kriegler, E.; Edmonds, J.; O'neill, B.C.; Fujimori, S.; Bauer, N.; Calvin, K.; Dellink, R.; Fricko, O.; et al. The Shared Socioeconomic Pathways and their energy, land use, and greenhouse gas emissions implications: An overview. *G. Environ. Chang.* **2017**, *42*, 153–168. [CrossRef]

36. Gidden, M.; Riahi, K.; Smith, S.; Fujimori, S.; Luderer, G.; Kriegler, E.; van Vuuren, D.P.; van den Berg, M.; Feng, L.; Klein, D.; et al. Global emissions pathways under different socioeconomic scenarios for use in CMIP6: A dataset of harmonized emissions trajectories through the end of the century. *Geosci. Model Dev.* **2019**, *12*, 1443–1475. [CrossRef]

37. Ault, T.R.; Cole, J.E.; Overpeck, J.T.; Pederson, G.T.; Meko, D.M. Assessing the risk of persistent drought usingclimate model simulations and paleoclimate data. *J. Clim.* **2014**, *27*, 7529–7549. [CrossRef]

38. Williams, A.P.; Seager, R.; Abatzoglou, J.T.; Cook, B.I.; Smerdon, J.E.; Cook, E.R. Contribution of anthropogenic warming to California drought during 2012–2014. *Geophys. Res. Lett.* **2015**, *42*, 6819–6828. [CrossRef]

39. Rauscher, S.A.; Giorgi, F.; Diffenbaugh, N.S.; Seth, A. Extension and intensification of the Meso-American mid-summer drought in the twenty-first century. *Clim. Dyn.* **2008**, *31*, 551–571. [CrossRef]

40. Ryu, J.-H.; Hayhoe, K. Understanding the sources of Caribbean precipitation biases in CMIP3 and CMIP5 simulations. *Clim. Dyn.* **2014**, *42*, 3233–3252. [CrossRef]

41. Taylor, M.A.; Whyte, F.S.; Stephenson, T.S.; Campbell, J.D. Why dry? Investigating the future evolution of the Caribbean Low Level Jet to explain projected Caribbean drying. *Int. J. Climatol.* **2013**, *33*, 784–792. [CrossRef]

42. Amador, J.A. A climatic feature of the tropical Americas: The trade wind easterly jet. *Tóp. Meteorol. Oceanogr.* **1998**, *5*, 91–102.

43. Swann, A.L.S.; Hoffman, F.M.; Koven, C.D.; Randerson, J.T. Plant responses to increasing CO2 reduce estimates of climate impacts on drought severity. *Proc. Nat. Acad. Sci. USA* **2016**, *113*, 10019–10024. [CrossRef]

44. Trugman, A.T.; Medvigy, D.; Mankin, J.S.; Anderegg, W.R.L. Soil moisture stress as a major driver of carbon cycle uncertainty. *Geophys. Res. Lett.* **2018**, *45*, 6495–6503. [CrossRef]

45. Cook, B.I.; Mankin, J.S.; Marvel, K.; Williams, A.P.; Smerdon, J.E.; Anchukaitis, K.J. Twenty-first century drought projections in the CMIP6 forcing scenarios. *Earth's Future* **2020**, *8*, e2019EF001461. [CrossRef]

46. Scoccimarro, E.; Gualdi, S. Heavy Daily Precipitation Events in the CMIP6 Worst-Case Scenario: Projected Twenty-First-Century Changes. *J. Clim.* **2020**, *33*, 7631–7642. [CrossRef]

47. US Global Change Research Program. Global Climate Change Impacts in the United States. 2009. Available online: https://nca2009.globalchange.gov/islands/index.html#footnote7_n3w79p3 (accessed on 1 October 2020).

48. Centella-Artola, A.; Taylor, M.A.; Bezanilla-Morlot, A.; Martinez-Castro, D.; Campbell, J.D.; Stephenson, T.S.; Vichot, A. Assessing the effect of domain size over the Caribbean region using the PRECIS regional climate model. *Clim. Dyn.* **2015**, *44*, 1901–1918. [CrossRef]

49. Martínez-Castro, D.; Vichot-Llano, A.; Bezanilla-Morlot, A.; Centella-Artola, A.; Campbell, J.; Viloria-Holguin, C. Performance of RegCM-4.3 over the Caribbean region using different configurations of the Tiedtke convective parameterization scheme. *Rev. Climatol.* **2016**, *16*, 77–98.

50. Vichot-Llano, A.; Martinez-Castro, D.; Giorgi, F.; Bezanilla-Morlot, A.; Centella-Artola, A. Comparison of GCM and RCM simulated precipitation and temperature over Central America and the Caribbean. *Theor. Appl. Climatol.* **2020**. [CrossRef]

51. Navarro-Racines, C.; Tarapues, J.; Thornton, P.; Jarvis, A.; Ramirez-Villegas, J. High-resolution and bias-corrected CMIP5 projections for climate change impact assessments. *Sci. Data* **2020**, *7*, 7. [CrossRef] [PubMed]

52. Sobel, A.H.; Burleyson, C.D.; Yuter, S.E. Rain on small tropical islands. *J. Geophys. Res.* **2011**, *116*, D08102. [CrossRef]